IEEE Access
Multidisciplinary | Rapid Review | Open Access Journal

Received February 7, 2021, accepted March 3, 2021, date of publication March 8, 2021, date of current version March 23, 2021.

Digital Object Identifier 10.1109/ACCESS.2021.3064212

High-Impedance Wireless Power Transfer Transmitter Coils for Freely Positioning Receivers

MASOUD SHARIFIAN MAZRAEH MOLLAEI, PRASAD JAYATHURATHNAGE, (Member, IEEE), SERGEI A. TRETYAKOV, (Fellow, IEEE), AND CONSTANTIN R. SIMOVSKI
Department of Electronics and Nanotechnology, Aalto University, 02150 Espoo, Finland

Corresponding author: Masoud Sharifian Mazraeh Mollaei (masoud.2.sharifianmazraehmollaei@aalto.fi)

This work was supported in part by the Academy of Finland Postdoctoral researcher under Grant 333479 and in part by the Business Finland Research-to-business under Grant 1527/31/2020.

ABSTRACT In this letter, a wireless power transfer (WPT) system based on two high-impedance coil (HIC) – cable loop antennas with a modified shield – as transmitters (Tx)s and a spiral coil as a receiver (Rx) is proposed and discussed. Utilizing features of HIC at its parallel-circuit resonance frequency, we design the Tx in a way that in the absence of the Rx, the input impedance of the Tx is very high compared to the case when the Rx is near the Tx. This feature offers a possibility for free positioning of the Rx over an array of Txs and auto self-activation and de-activation of the Txs, leading to highly efficient performance. To verify the proposed solution, we have designed, fabricated, and experimentally tested a WPT system based on two HICs as Txs and one Rx. The proposed system operates in a high-frequency range (around 280 MHz) in the near-field coupling regime. The measured averaged efficiency of the prototype is higher than 93%. The proposed system is simple, cheap, and does not require any control circuit system for tuning the system when the receiver position changes.

INDEX TERMS Free positioning, high impedance, shielded loop antennas, wireless power transfer.

I. INTRODUCTION

Recently, the use of wireless power transfer (WPT) technology has been growing in many applications such as consumer electronics, medical implant devices, and electric vehicles. Yet, there are several technical obstacles and limitations required to be overcome for a wide and successful utilization of the WPT technology. In particular, there are limiting requirements of perfect alignment of the transmitter (Tx) and receiver (Rx). Realizing WPT systems where Rx can be freely positioned is still a challenge, as that requires tracking the Rx position, proper Tx activation in the presence of Rx, and Tx de-activation in the absence of Rx.

To overcome these limitations, many techniques have been proposed which can be categorized into two main types: the use of large Txs to generate a uniform magnetic field over a large area and the employment of multiple Txs [1]–[4]. However, the first technique suffers from low efficiency because of weak coupling between Tx and Rx [1], [5]. The second technique suffers from complexity. To reduce the complexity of devices with multiple Txs, researchers usually excite all the Txs simultaneously [6]–[8]. However, because different Txs have different coupling levels to the Rx, an additional control circuit is anyway required for deactivation of weakly coupled Txs (otherwise the efficiency of the power transfer would be low) [9]–[13]. As an alternative, a multi-Tx free-positioning WPT system is proposed in [14] that is capable of self-tuning the currents in each Tx coil depending on the receiver position. In that approach, a layer of Tx coils and repeater coils is introduced, forming self-tuning power channels. However, applicability of this approach is limited to low working frequencies, while the use of free-positioning WPT systems in multi-MHz frequencies has become an increasingly demanding application requirement [15].

In this paper, we propose a self-tuning WPT system in which power channeling automatically occurs between the nearest Tx and Rx coils without any additional control circuits. The idea is to design a Tx coil in a way that if an Rx is located above it, the power is transferred between them, while if the Rx is not present near the Tx, the Tx automatically deactivates itself due to its characteristic features. Due to this property, the position of the receiver can freely change while the performance of the system remains highly efficient because the ineffective Tx coils that are far away from the Rx are automatically deactivated. In this article, we show that this property can be realized if the input impedance

The associate editor coordinating the review of this manuscript and approving it for publication was Davide Ramaccia.

of the transmitting coil strongly depends on the presence or absence of the receiver device in the vicinity of the transmitter.

The suggested approach is inspired by the known idea of so-called "high impedance coil" (HIC) based on shielded loop antennas [16]. In that work, the performance of basic HIC and means to change its resonance frequency are comprehensively studied. The basic HIC is made of a coaxial cable loop coil which has a gap in its shield at the position opposite to the antenna input port, while the shield is continuous at the antenna port position (there is a small hole in the shield at the position of the feeding point from where the source is connected to the inner wire). By cutting additional symmetric gaps in the shield or/and the inner wire, the resonance frequency of the coil can be tuned. In the circuit model of the basic HIC, the inductive impedance due to the outer surface of the shield is connected to the antenna port through two transmission lines constituted of the inner wire and the inner surface of the shield. At the resonance frequency, the input impedance of this coil is very high because the resonance is a parallel-circuit one.

In this work, our aim is to design the system so that the input impedance of the HIC in the presence of a nearby receiver would become small. In this case, all Txs that have no nearby receivers are self-deactivated, because the current through the high-impedance coil is very small. But as soon as an Rx appears in the vicinity of a Tx coil, its impedance drops, and current starts to flow through the Tx, ensuring its self-actuation. This property can be realized because when another loop antenna is located near the HIC, the total inductive impedance on the outer surface of the shield changes due to coupling between the Tx and Rx. This change detunes the Tx from the resonance, and the absolute value of the impedance becomes relatively low as compared to the resonant case.

II. THEORY AND DESIGN

A. THEORY

Figure 1(a) shows the proposed HIC positioned in free space. There are three gaps in the shield, one at the top of the coil and two symmetric gaps on the sides. The inner wire is continuous except the antenna port. Z_{in} is the input impedance of the HIC (the inner wire is shown by a dashed line to indicate that this wire is inside the shield). The basic HIC proposed in [16] has only one gap. In the modified HIC proposed in this work we introduce two additional symmetrically positioned gaps to shift the resonance to a higher frequency. At the resonance frequency, due to the transformation of the outer surface of the shield impedance $Z_{\rm sh} = R_{\rm rad} + j\omega L_{\rm shield}$ ($R_{\rm rad}$ is the radiation resistance, and $L_{\rm shield}$ is the outer surface inductance) to the feeding point, the input impedance of the coil becomes very high. In this case, if we assume that a 50 Ω source is connected to the coil through a 50 Ω cable, then there will be a huge mismatch between 50 Ω and the input impedance of the coil, meaning that the power will be not delivered to the coil.

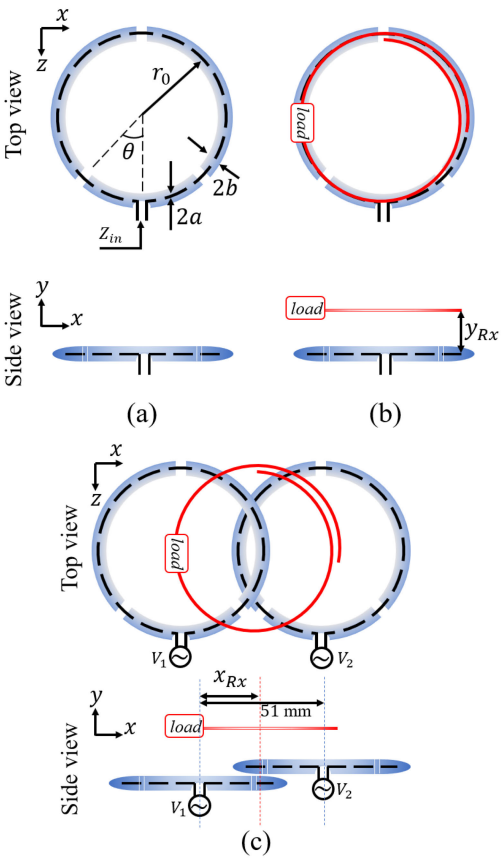

FIGURE 1. Schematic view of: (a) the proposed transmitter in free space, (b) the proposed transmitter in presence of the proposed receiver, and (c) the WPT system based on two overlapped transmitters and a receiver positioned above them.

By locating an Rx near the modified-HIC (as shown in Fig. 1(b)), the mutual impedance between the HIC and the Rx is added to the circuit. In this case, the modified impedance of the shield outer surface is $Z_{\rm sh} = R_{\rm rad} + j\omega L_{\rm shield} + Z_M$, where Z_M is the reflected impedance due to the mutual inductance L_M. The reflected impedance is the impedance seen by the Tx shield due to the presence of the receiver, and it reads $Z_M = (\omega L_M)^2/Z_{Rx}$, where Z_{Rx} is the impedance of the receiver [17]. Impedance $Z_{\rm sh}$ is transformed to the feeding point, and the transformed value is much smaller than in the case without the Rx. Therefore, the power delivered from the source to the Tx is indeed self-tuning depending on the mutual coupling between Tx and Rx. If the receiver is close to the Tx (with stronger mutual coupling), the power extracted from the power source is much higher than in the case when the receiver is far away. This self-tuning characteristic is highly desirable in multi-Tx WPT scenario (this conclusion is verified in Section IV).

With these insights about the performance of modified HIC, we study a two-Tx WPT system where two HICs are placed next to each other as the Txs. We name the two transmitting coils Tx1 and Tx2. We position the two loops with a small overlap in order to decouple them from each

other. Figure 1(c) shows the WPT structure with two Tx coils and an Rx coil over the Tx array.

B. TRANSMITTERS DESIGN

The resonance frequency of HICs is determined by the size of the coil, the characteristic impedance of the coaxial cable, and the positions of the gaps in the shield. In order to reduce the radiation resistance of the coil which leads to parasitic radiation, we reduce the size of the TXs as much as possible. Moreover, due to a small size compared to the operating wavelength, the current over the outer surface of the shield is nearly uniform, which allows us to decouple the Txs by overlapping them. Considering bending limitation of usual coaxial cables, the radius of the Tx should be larger than about 25 mm. Moreover, to confirm the possibility of tuning the resonance frequency of the coil by adding symmetric gaps, we have added two gaps at the angle θ, as shown in Fig. 1(a) (a parametric study of shifting the resonance frequency by changing the position of these added gaps is presented in [16]). Other geometric parameters of the structure are also shown in Fig. 1.

C. RECEIVER DESIGN

The Rx must be designed so that when the mutual inductance between the Rx and Tx increases, the input impedance at the port of Tx decreases, otherwise the system does not perform as desired. This property is realized if the Rx is a coil whose resonance is a series-circuit resonance. To increase coupling, instead of a single-loop coil we use a spiral coil as the Rx, where the load is in the series connection to the capacitance and inductance of the circuit model of the spiral. This spiral coil (Rx) is shown in Fig. 1. Using a spiral coil allows us to tune the resonance frequency of the coil easily, moreover, not having any lumped elements, this receiver can operate at high power. Proper design of the load terminal is important to achieve the desired characteristics. For example, if the load is connected between the ending points of the spiral, then the circuit model of the coil exhibits a parallel-circuit resonance at the lowest resonance frequency, making it not suitable for our purpose. When the load is connected to the spiral in series (as shown in Fig. 1(b)), then the first resonance of the coil is a series-circuit resonance, which suits our goals. In our design, we use the same radius for both Txs and Rx, the load is 50 Ω, and the position of the receiver in the xy-plane is indicated by the coordinates x_{Rx} and y_{Rx} in Fig. 1.

III. VERIFICATION METHOD

A. NUMERICAL SIMULATION

Full-wave simulations have been carried out using CST Microwave Studio, both in the frequency and time domains. These simulations allowed us to numerically find the following parameters:

- The input impedance of the Tx in the absence and presence of the Rx.
- The input impedance of both Tx coils (Tx1 and Tx2) in the presence of the Rx while the position of the Rx changes above Txs.
- The power extracted from the source and the power received by the load for varying positions of the Rx.
- Efficiency of the designed WPT system with respect to the position of the Rx.

To calculate the change of the input impedance in the absence and presence of the Rx, a lumped voltage source is directly connected to the input port of the Tx, as shown in Fig. 1(a). First, the self-impedance of the transmitter is calculated; after that, the receiver is located above the transmitter and the input impedance of the transmitter is recalculated ($y_{Rx} = 10$ mm in this simulation). These results numerically confirm the theoretical results (as will be discussed in the next section) about the change of the Tx input impedance.

Next, we simulated the performance of two Txs in the presence of the Rx. In this case, two voltage sources are connected to the ports of Tx1 and Tx2, and the Rx is located above them. The two Txs are decoupled to mitigate power flow between Txs. The percentage of overlap between the Txs is slightly dependent on the position of the Rx. In our simulation setup, we located the Rx above and in between the Txs and then numerically found the optimal overlapping percentage ($y_{Rx} = 10$ mm and $x_{Rx} = 25.5$ mm). After defining the reference decoupled case, to verify the proposed method, we numerically calculated the input impedance of each Tx while the position of the Rx changed. Moreover, the delivered power to each Tx, the power received by the load, and, finally, the efficiency of the system were calculated. In the simulation, we monitored the currents and voltage at the ports of the Txs and the 50 Ω load in the Rx. Knowing both voltage and current, we calculated the input impedance of each Tx, the actually delivered powers to the Txs, the power received by the load, and the efficiency of the system. Note that the efficiency is defined as the ratio between the actual power received by the Rx to the power extracted from the source.

In all these simulations, the inner wire and the shield of the coaxial cable are made of copper, the relative permittivity of the coaxial cable filling is $\epsilon_r = 2.2$, and the other parameters of the transmitters are $r_0 = 30$ mm, $b = 1.3$ mm, $a = 0.5$ mm, $\theta = 20°$. The thickness of the shield is 0.1 mm, and the length of the gaps is 3 mm (all the parameters are shown in Fig. 1). The Rx coil is also made of copper, the radius is 30 mm, the number of turns is 1.25, the diameter of the wire is 0.5 mm, and the load is 50 Ω. With these parameters, we numerically found that Txs need to be overlapped by 9 mm, meaning that the distance between Txs is 51 mm. Moreover, Tx2 is located above Tx1, and the distance between their shields is 1 mm. $y_{Rx} = 10$ mm, and the receiver position along the x-axis varies, with the values $x_{Rx} = 0, 8.5, 17, 25.5, 34, 42.5$ mm, and 51 mm ($x_{Rx} = 51$ mm refers to the case when the receiver is exactly above Tx2).

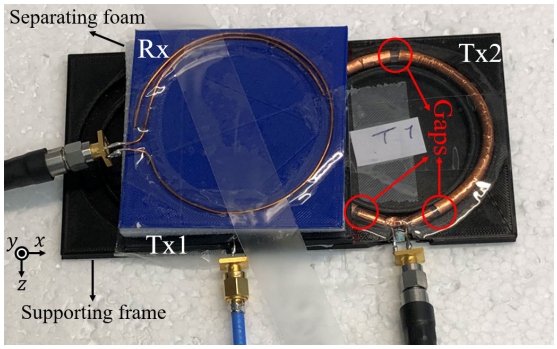

FIGURE 2. Picture of the fabricated system for experimental verification. Two transmitters are partially overlapped and fixed with a supporting frame. The space between the transmitters and receiver is filled by a separating foam that keeps the distance fixed during measurement.

B. MEASUREMENT SETUP

To validate the theory and simulation results, we fabricated two proposed Tx and one Rx. Figure 2 shows the fabricated system and the coil arrangement of the measurement setup. To fabricate Txs, we used the coaxial cable *Bedea 1085 RG 59* ($a = 0.2875$ mm and $\epsilon_r = 2.2$) and replaced the shield with a copper tape. The gaps in the shield are shown by red circles in Fig. 2. In the experiment, two symmetric gaps over the shield are located at $\theta = 18°$. To fabricate the Rx, we used a copper wire with 0.5 mm diameter and 1.5 turns, and manually adjusted the gap between the turns to tune the resonance frequency of the Rx to the required frequency. The other parameters are the same as those used in the simulations. *Rohde Schwarz ZND* Vector Network Analyzer (VNA) was used to study the performance of the structure. The impedance of the port connected to the Rx plays the role of the 50 Ω load in the receiver.

With the experimental study, we aimed to analyze: (i) the input impedance of the designed Tx in the absence and presence of the Rx (only one Tx is present); (ii) the power delivered to each Tx and the Rx, and the efficiency of the system with respect to the position of the Rx (two Txs are overlapped, and the Rx is positioned above them). The input impedance of one Tx is directly measured using the VNA. To find the transferred powers and the efficiency, we measured the S-parameters of the system. The powers delivered to Tx1 and Tx2 are found as

$$P_{Tx1} = 1 - |S_{11}|^2 \tag{1}$$

and

$$P_{Tx2} = 1 - |S_{22}|^2. \tag{2}$$

The total received power reads

$$P_{Rx} = |S_{31} + S_{32}|^2, \tag{3}$$

and the efficiency is defined as

$$\eta = \frac{P_{Rx}}{P_{Tx1} + P_{Tx2}}, \tag{4}$$

where the indices 1, 2, and 3 stand for Tx1, Tx2, and Rx, respectively. For the measurements, we located the Rx at $y_{Rx} = 10$ mm and $x_{Rx} = 0$, 12.25, 25.5, 37.75, and 52 mm.

IV. RESULTS AND DISCUSSION

Figures 3(a) and (b) compare numerical and experimental results for the input impedance of the proposed Tx in the absence and presence of the Rx. In all the cases, the input impedance of the Tx shows a parallel-circuit resonance. The input impedance decreases significantly when the Rx is present. For example, the input impedance changes from 200 $k\Omega$ to 400 Ω at 250 MHz in simulation and from 7 $k\Omega$ to 350 Ω in measurements. The maximum of the WPT efficiency occurs at a higher frequency compared to the individual resonance frequency of the transmitter and receiver (250 MHz). The reason of this frequency shift is the strong coupling of our Rx with Tx1. This coupling makes the pair of antennas (Tx1 and Rx) a dual-resonant circuit with two normal modes. The lower normal mode resonates at 185 MHz (as mentioned above) and the higher normal mode resonates at 340 MHz. Unlike the usual coupled circuits where the resonances of the coupled modes are series ones, these resonances correspond to very high values of the input impedance of Tx1 because Tx1 is a HIC. The frequency dispersion of the input impedance of Tx1 in presence of Rx is shown in Fig. 3(a). We see in this plot that in between these two parallel resonances there is a series corresponding to the best matching of our Tx.

Although the simulated impedances are higher, and there is a frequency shift as compared to the experimental data, these results fully confirm that the input impedance of the proposed Tx drastically decreases in the presence of the Rx. In fact, the discrepancies are mainly due to dissipation losses in materials used in the experiment (especially the copper tape). Moreover, the presence of the measurement setup elements (namely, the supporting frame and separating foam) affects the mutual coupling between the Tx and Rx which leads to some difference between the measurements and simulations.

Figure 3(c) shows the experimentally measured input impedances of Tx1 and Tx2 with respect to the position of the Rx ($y_{Rx} = 10$ mm is fixed, and x_{Rx} varies between 0 and 51 mm). When the Rx is above Tx1 (at $x_{Rx} = 0$), the input impedance of Tx1 is much lower compared to that of Tx2. In this situation, the mismatch between the 50 Ω cable and the input impedance of Tx1 is much lower than the mismatch between the same cable and Tx2, meaning that power is properly extracted by Tx1 from source 1 while the power extracted by Tx2 from source 2 is negligible. When the Rx is moving toward Tx2, the input impedances of Tx1 and Tx2 increase and decrease, respectively. As such, the power extracted by any Tx decreases when the Rx is moving away from it and the power increases when the Rx is moving closer to it. It means that the power extracted by two Txs are self-tuning depending on the Rx position. In other words, as long as the Rx is close to Tx2, more power is extracted from

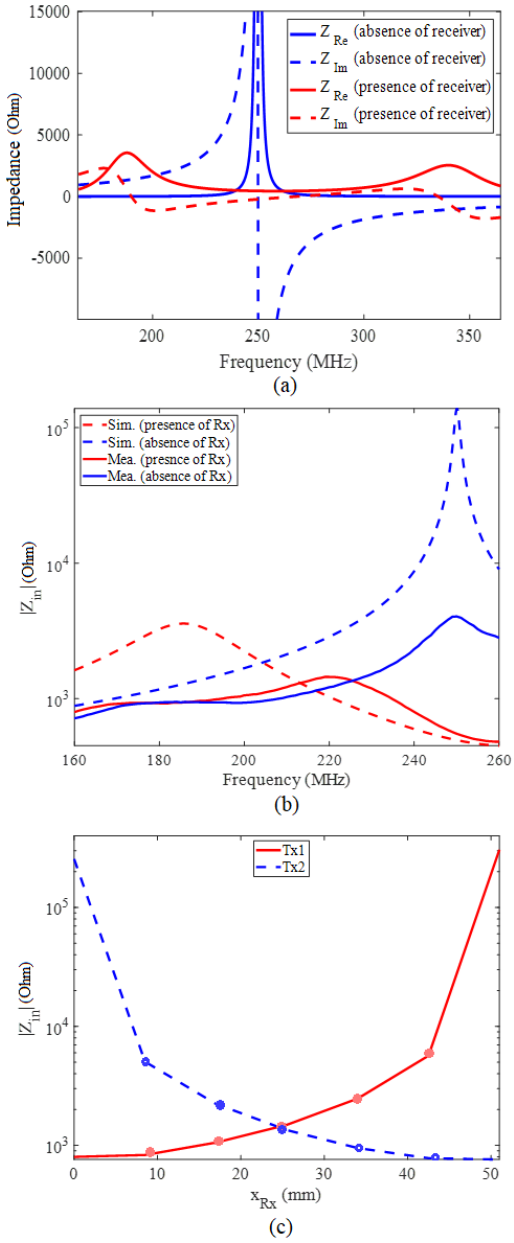

FIGURE 3. (a) Real and imaginary parts of the input impedance of the proposed transmitter in the absence and presence of the receiver (numerical results); (b) experimental results versus numerical ones for the absolute value of the input impedance. (c) The absolute values of the input impedances of both transmitters shown in Fig. 1(c) with respect to the receiver position (numerical results).

source 2 while the power extracted from source 1 is small. This proves that the proposed WPT system can be used to charge freely positioned Rxs above an array of Txs. A small asymmetry between the variation of the red and blue lines in this figure is due to the fact that Tx2 is located slightly above Tx1 (to enable Txs overlapping for coil decoupling).

Next, the performance indicators of the proposed and tested WPT system are presented. In Fig. 4, the numerically obtained efficiency of the system, shown in Fig. 1(c), is presented for a wide range of frequencies. In this figure, we show the efficiency of the system based on the formulas

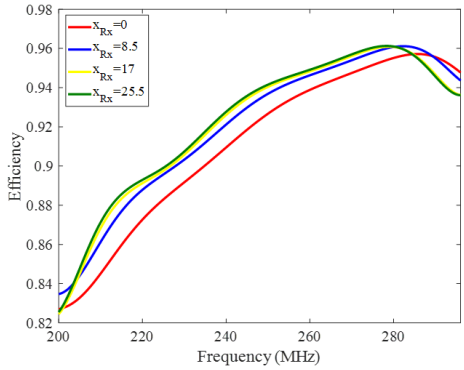

FIGURE 4. Efficiency of the system with respect to the position of the receiver over a wide frequency range (numerical results). The maximum efficiency occurs at 280 MHz (while the resonance frequency of a single Tx occurs at 250 MHz) due to strong coupling of our Rx with Tx1.

of the previous section. The position of the Rx is varying from $x_{Rx} = 0$ to 25.5 mm.

Figure 5(a) shows the efficiency of the system at 280 MHz with respect to the Rx position. Simulated and experimental results are in good agreement. The disparity between the simulation and experimental results may be explained by the effects of the supporting frame, losses in the connectors, and additional resistance of the copper tape used as the shield of the Txs coils. Moreover, when x_{Rx} is larger than 25.5 mm, the Rx is located mostly over Tx2. Because Tx2 is slightly over Tx1, the power transferred from Tx2 is received better by the Rx, meaning that the efficiency is slightly higher in this case. It is important that the efficiency of the system is high and almost constant throughout all the receiver positions.

Figure 5(b) shows the extracted power by each Tx, the total extracted power from the sources, and the power received by the load for varying positions of the Rx. The overall performance of the system is as expected: When the Rx is above Tx1, Tx1 is active and sends power to the load, while Tx2 is deactivated automatically; when the Rx is moved towards Tx2, the power extracted from source 1 decreases and the power extracted from source 2 increases. A slight disagreement between the simulated and measured might have the same reason as explained above. Again, what is important is that the received power is sufficiently constant for all Rx positions.

To further check the feature of freely positioning the Rx over the Txs, we also rotated the Rx around its axis and remeasured already reported results. Based on the numerical and experimental results obtained with rotations of the Rx, the performance of the structure remains the same in terms of the received power and efficiency which proves the feature of freely positioning of the Rx.

Note that we verified the proposed concept using two–Tx WPT system at low power level (using a network analyzer) in a laboratory prototype, however, in principle, the proposed design can be used in multi-Tx scenario with higher power capabilities. For example, multiple Tx coils can be placed in a form of a two-dimensional array to enable large area power transfer. As we do not introduce any lumped tuning

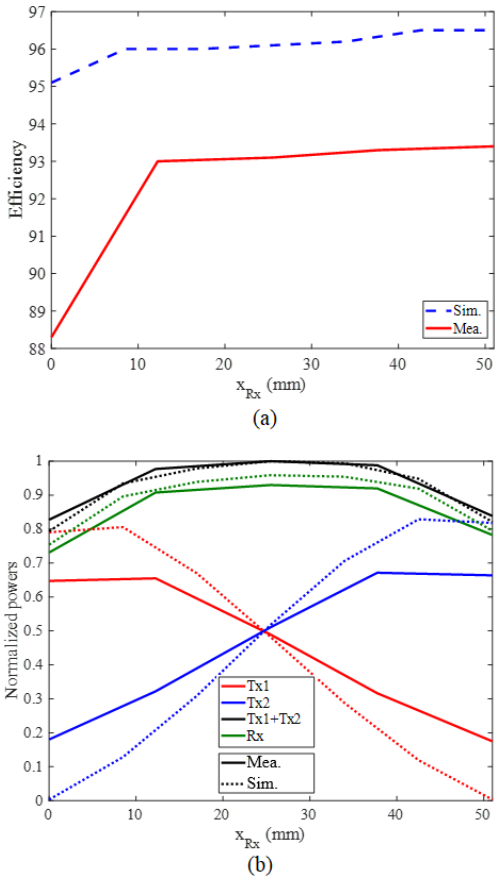

FIGURE 5. (a) Numerical and experimental results for the system efficiency with respect to the position of the receiver at frequency 280 MHz. (b) The powers delivered to the transmitters and the power received by the load normalized to the maximum total power extracted from the sources with respect to the position of the receiver. Solid lines represent the experimental results and dashed lines represent the numerical results.

capacitors (or inductors) the power rating of the WPT device is mainly determined by the rated current of the windings. We believe that the power level of the coil design of this article can easily be up to few tens of Watts, while higher power can be achieved by carefully designing the coil parameters such as, size of the coil and thickness of copper. Therefore, it is apparent that the proposed structure can be useful in a wide range of WPT applications.

V. CONCLUSION

A self-tuning multi-Tx WPT system is proposed for applications with freely positioned receivers. In this system, depending on the position of the Rx, the nearest Tx is activated and the other Txs are deactivated automatically, without any control system. This feature ensures highly efficient WPT performance. Numerical and experimental results prove that the efficiency of the system is about 93%, and the received power remains almost the same while the position of the Rx above the Tx array changes.

REFERENCES

[1] X. Liu and S. Y. Hui, "Optimal design of a hybrid winding structure for planar contactless battery charging platform," *IEEE Trans. Power Electron.*, vol. 23, no. 1, pp. 455–463, Jan. 2008.

[2] U.-M. Jow and M. Ghovanloo, "Geometrical design of a scalable overlapping planar spiral coil array to generate a homogeneous magnetic field," *IEEE Trans. Magn.*, vol. 49, no. 6, pp. 2933–2945, Jun. 2013.

[3] W. X. Zhong, X. Liu, and S. Y. R. Hui, "A novel single-layer winding array and receiver coil structure for contactless battery charging systems with free-positioning and localized charging features," *IEEE Trans. Ind. Electron.*, vol. 58, no. 9, pp. 4136–4144, Sep. 2011.

[4] C. C. Mi, G. Buja, S. Y. Choi, and C. T. Rim, "Modern advances in wireless power transfer systems for roadway powered electric vehicles," *IEEE Trans. Ind. Electron.*, vol. 63, no. 10, pp. 6533–6545, Oct. 2016.

[5] S. A. Mirbozorgi, H. Bahrami, M. Sawan, and B. Gosselin, "A smart multicoil inductively coupled array for wireless power transmission," *IEEE Trans. Ind. Electron.*, vol. 61, no. 11, pp. 6061–6070, Nov. 2014.

[6] S. A. Mirbozorgi, H. Bahrami, M. Sawan, and B. Gosselin, "A smart cage with uniform wireless power distribution in 3D for enabling long-term experiments with freely moving animals," *IEEE Trans. Biomed. Circuits Syst.*, vol. 10, no. 2, pp. 424–434, Apr. 2016.

[7] F. Jolani, Y.-Q. Yu, and Z. Chen, "A planar magnetically-coupled resonant wireless power transfer using array of resonators for efficiency enhancement," in *IEEE MTT-S Int. Microw. Symp. Dig.*, May 2015, pp. 1–4.

[8] J. W. Kim, H.-C. Son, D.-H. Kim, J.-R. Yang, K.-H. Kim, K.-M. Lee, and Y.-J. Park, "Wireless power transfer for free positioning using compact planar multiple self-resonators," in *IEEE MTT-S Int. Microw. Symp. Dig.*, May 2012, pp. 127–130.

[9] S. Y. Hui, "Planar wireless charging technology for portable electronic products and Qi," *Proc. IEEE*, vol. 101, no. 6, pp. 1290–1301, Jun. 2013.

[10] A. Pacini, A. Costanzo, S. Aldhaher, and P. D. Mitcheson, "Load- and position-independent moving MHz WPT system based on GaN-distributed current sources," *IEEE Trans. Microw. Theory Techn.*, vol. 65, no. 12, pp. 5367–5376, Dec. 2017.

[11] W. Kim and D. Ahn, "Efficient deactivation of unused LCC inverter for multiple transmitter wireless power transfer," *IET Power Electron.*, vol. 12, no. 1, pp. 72–82, Jan. 2019.

[12] X. Dai, X. Li, Y. Li, and A. P. Hu, "Maximum efficiency tracking for wireless power transfer systems with dynamic coupling coefficient estimation," *IEEE Trans. Power Electron.*, vol. 33, no. 6, pp. 5005–5015, Jun. 2018.

[13] V. Jiwariyavej, T. Imura, and Y. Hori, "Coupling coefficients estimation of wireless power transfer system via magnetic resonance coupling using information from either side of the system," *IEEE J. Emerg. Sel. Topics Power Electron.*, vol. 3, no. 1, pp. 191–200, Mar. 2015.

[14] X. Dang, P. Jayathurathnage, S. A. Tretyakov, and C. R. Simovski, "Self-tuning multi-transmitter wireless power transfer to freely positioned receivers," *IEEE Access*, vol. 8, pp. 119940–119950, 2020.

[15] J. M. Arteaga, S. Aldhaher, G. Kkelis, C. Kwan, D. C. Yates, and P. D. Mitcheson, "Dynamic capabilities of multi-MHz inductive power transfer systems demonstrated with batteryless drones," *IEEE Trans. Power Electron.*, vol. 34, no. 6, pp. 5093–5104, Jun. 2019.

[16] M. S. M. Mollaei, C. C. Van Leeuwen, A. J. E. Raaijmakers, and C. R. Simovski, "Analysis of high impedance coils both in transmission and reception regimes," *IEEE Access*, vol. 8, pp. 129754–129762, Jul. 2020.

[17] C.-S. Wang, G. A. Covic, and O. H. Stielau, "Power transfer capability and bifurcation phenomena of loosely coupled inductive power transfer systems," *IEEE Trans. Ind. Electron.*, vol. 51, no. 1, pp. 148–157, Feb. 2004.

MASOUD SHARIFIAN MAZRAEH MOLLAEI was born in Tehran, Iran, in 1989. He received the B.Sc. degree in electrical engineering from Imam Khomeyni International University, Qazvin, Iran, in 2013, and the M.Sc. degree in electrical engineering from the Iran University of Science and Technology (IUST), Tehran, in 2016. He is currently pursuing the Ph.D. degree with the Department of Electronics and Nanotechnology, Aalto University, Espoo, Finland, where he has been developing theoretical and experimental techniques for ultra-high field magnetic resonance imaging.

His current research interests include array antennas, antenna decoupling, metamaterials, and photonics. The aim of his thesis is to introduce a novel method for decoupling dipole and loop antenna arrays for 7 T MRI.

PRASAD JAYATHURATHNAGE (Member, IEEE) received the B.Sc. degree in electronics and telecommunications engineering from the University of Moratuwa, Moratuwa, Sri Lanka, in 2009, and the Ph.D. degree in electrical and electronics engineering from Nanyang Technological University, Singapore, in 2017. He is currently a Postdoctoral Researcher with Aalto University, Espoo, Finland. His research interests include high-frequency power converters, wireless power transfer, and biomedical implants.

SERGEI A. TRETYAKOV (Fellow, IEEE) received the Dipl. Engineer-Physicist, Candidate of Sciences (Ph.D.), and D.Sc. degrees in radiophysics from Saint Petersburg State Technical University, Saint Petersburg, Russia, in 1980, 1987, and 1995, respectively. From 1980 to 2000, he was with the Department of Radiophysics, Saint Petersburg State Technical University. He is currently a Professor of radio science with the Department of Electronics and Nanoengineering, Aalto University, Espoo, Finland. He has authored or coauthored 5 research monographs and more than 300 journal articles. His current research interests include electromagnetic field theory, complex media electromagnetics, metamaterials, and microwave engineering. He served as the Chairman for the Saint Petersburg IEEE Electron Devices/Microwave Theory and the Techniques/Antennas and Propagation Chapter, from 1995 to 1998, the General Chair for the International Congress Series on Advanced Electromagnetic Materials in Microwaves and Optics (Metamaterials), and the President for the Virtual Institute for Artificial Electromagnetic Materials and Metamaterials (Metamorphose VI), from 2007 to 2013.

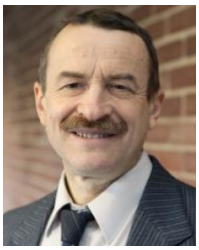

CONSTANTIN R. SIMOVSKI was born in Leningrad, Saint Petersburg, Russia, in December 1957. He received the Dipl. Eng. degree (by Research) in radio engineering, the Ph.D. degree in electromagnetic theory, and the D.Sc. degree from St. Petersburg State Polytechnic University (formerly the Leningrad Polytechnic Institute, and State Technical University), Saint Petersburg, in 1980, 1986, and 2000, respectively.

From 1980 to 1992, he was with the Soviet scientific and industrial firm ''Impulse.'' In 1986, he defended the Candidate of Science (Ph.D.) thesis (a study of the scattering of Earth waves in the mountains) with the Leningrad Polytechnic Institute. In 1992, he joined the St. Petersburg University of Information Technologies, Mechanics and Optics, as an Assistant where, from 1994 to 1995, he was an Assistant Professor, from 1995 to 2001, he was an Associate Professor, and since 2001, he has been a Full Professor. In 2000, he defended the thesis of Doctor of Sciences (a theory of 2-D and 3-D bianisotropic scattering arrays). Since 1999, he has been involved in the theory and applications of 2-D and 3-D electromagnetic band-gap structures for microwave and ultrashortwave antennas. His research interests include metamaterials for microwave and optical applications including optics of metal nanoparticles.